

Interferometer for Space Station Windows

Introduction

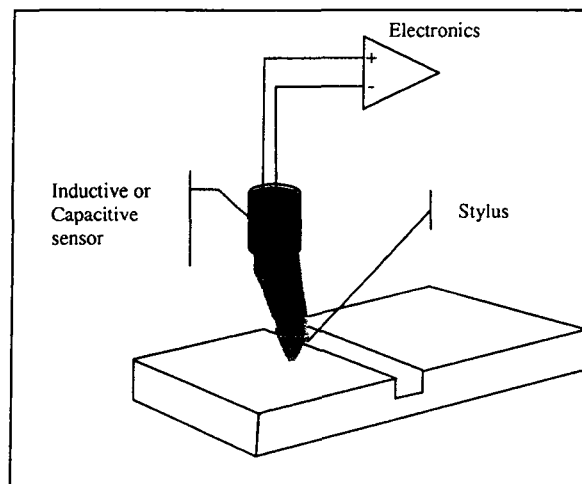
Inspection of space station windows for micrometeorite damage would be a difficult task insitu using current inspection techniques. Commercially available optical profilometers and inspection systems are relatively large, about the size of a desktop computer tower, and require a stable platform to inspect the test object. Also, many devices currently available are designed for a laboratory or controlled environments requiring external computer control. This paper presents an approach using a highly developed optical interferometer to inspect the windows from inside the space station itself using a self-contained hand held device. The interferometer would be capable as a minimum of detecting damage as small as one ten thousands of an inch in diameter and depth while interrogating a relatively large area. The current developmental state of this device is still in the proof of concept stage. The background section of this paper will discuss the current state of the art of profilometers as well as the desired configuration of the self-contained, hand held device. Then, a discussion of the developments and findings that will allow the configuration change with suggested approaches appearing in the proof of concept section.

Background

There are currently three major techniques of surface profilometry for measuring surface topography on the 1/10,000 inch scale. These methods are: 1) contact stylus, which can measure minute physical surface variations as a function of position. 2) confocal microscope or refocus microscope 3) optical interferometry. Each method will be briefly discussed here ending with a discussion of why an interferometric system was chosen as the sensing method.

A. Contact Stylus

The contact stylus method uses typically a diamond tipped stylus with a small surface area and radius to be dragged along the surface of the object under investigation with the vertical movements being registered by an inductive or capacitive detector (see figure 1).



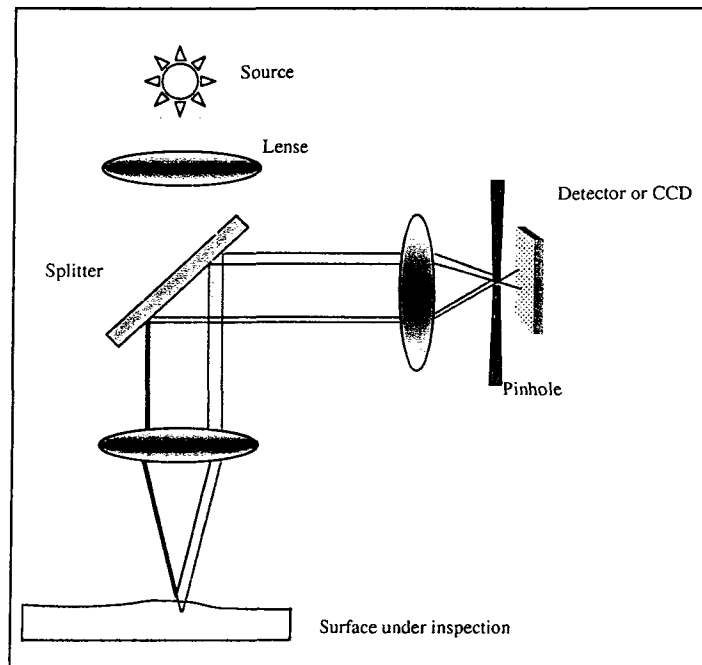
Typical performance specifications are:

Vertical range/ Resolution: 200-300 micro-inches/0.004micro-inches

Scan Speed: 80 micro-inches/second

Scan Length: 0.4 inches before object under test or sensor head must be moved must be moved

B. Confocal and Refocus Microscope



A laser or bright light source is used in order to get very high intensities, see figure 2. The light yellow line is directed through a lens to a beam splitter. From there, the light is directed to a lens or system of lenses, such as a microscope objective, for focusing on the area being interrogated. If the light is focused on the surface of the object the light returns to the lens (blue lines) and the beam splitter to be reflected to a third lens in front of a pin hole. This third lens is set so that it is focused on the pinhole allowing the light to travel through to the detector. If the light is not focused on the surface then the returned beam (red lines) returns to the third lens misaligned and does not pass through the pinhole and the signal is rejected. Systems are available that automatically focuses on the surface and makes a measurement. For areas larger than the scan area a technique known as stitching is used to “stitch” the measured areas together. More advanced systems can scan an area using a Nipcow disk for generating a image to a CCD camera, using a computer to build an image layer upon layer for the total height profile ⁽¹⁾. Recent advancements using Digital Micromirror Device (DMD), which allows rapid, lateral spatial scanning while a tunable source can allow rapid vertical scanning ⁽²⁾.

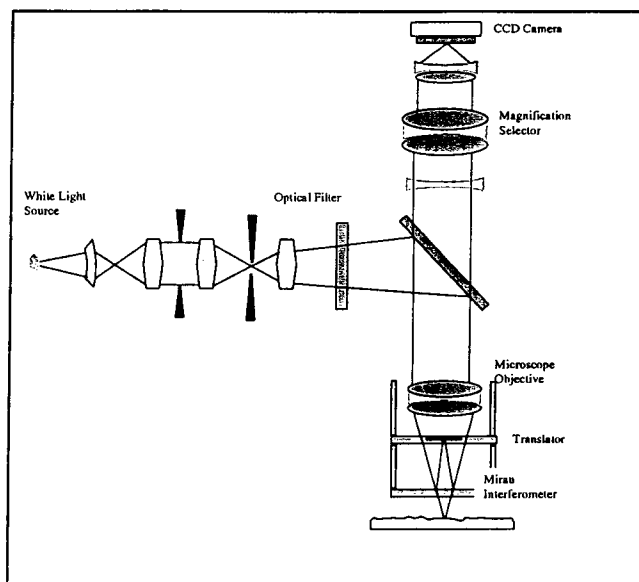
A refocus microscope is a microscope with a very narrow depth of focus. This allows objects at a very specific distance from the microscope to be in focus while objects at closer or further distances are out of focus. When the refocus microscope is placed over a defect; the height above the glass is controlled so that the focus is on the deepest portion of the damaged area. Then the focus made on the object surface, the delta in distance gives the maximum depth of the damage. This is usually a manual task and is very time consuming.

C. Optical Interferometry

Currently there are two major types or modes of optical profilers ⁽³⁾:

- 1) Phase shifting -for smooth surfaces typically up to $\frac{1}{4}$ wavelength with sub-nanometer resolution, (ref: 650nm wave length = 2.56×10^{-5} inches, or 100nm = 3.94×10^{-6} inches) and
- 2) Vertical scanning/ coherence sensing- for rougher surfaces, giving sub-nanometer resolution over several hundred microns of surface height

The phase shifting/ vertical scanning interferometer shown in figure 2, utilizes a bright white light source and pinhole disks to maintain spatial coherence (see left hand side of figure 2). An optical attenuator or optical filter is used when the interferometer is used in the phase shifting mode and is not used in the



vertical scanning/ coherence sensing mode. Filtered, narrow spectrum light is then passed to a microscope objective where light is focused and sent to the interferometer. Typically a Mirau interferometer is used when objective magnifications are between 10 and 50X, a Linnik interferometer is used for larger magnifications and a Michelson interferometer is used for low magnifications. Magnifications are needed to limit the field of view especially for rough surfaces so that a proper measurement can be made. Surfaces rougher than $\frac{1}{4}$ wavelength need to be focused to areas where the interrogation area maintains maximum changes less than $\frac{1}{4}$ wavelength. The interference signal or fringes are sent to a magnification selector and then to the sensor or CCD array.

In the vertical scanning/ coherence sensing mode the optical attenuator is removed allowing white light to enter the interferometer, this narrows the coherence length of the interferometer and allows surface peaks to be located^(4,5). Optical interferometers with narrow coherence functions can have very high signal to noise ratios (S/N) from areas of high coherence to areas of low coherence. Typical S/N values can be as high as 70 dB⁽⁶⁾. Both the process of vertical scanning and phase shifting modes can be automated and the data recorded and manipulated digitally to produce a signal representing the surface profile.

D. Desired Configuration for Space Station Window Inspection

It is desired to have a self-contained, turn-key, hand-held device. The device should have a simple user interface and not require the user to be an expert in the technology to measure the window damage. In order to reduce the size of the profilometer to a hand held unit the parts count must be held to a minimum especially the sensing elements. Secondly the unit needs have low power consumption since it is self contained and will run off of batteries. Finally, it is desired that the inspection be made from inside the space station, thus eliminating a contact stylus type profiler. Both the confocal and interferometric systems can be reduced to about the same parts count for the optics in a basic system, however the interferometric system is superior for two reasons:

- 1) An interferometer can utilize the entire returned signal from the interrogation beam where as the confocal microscope utilizes only the light that is in focus.

- 2) A window reflects only about 4% of the interrogation signal power, also the source is sent through an optical splitter twice allowing only 1% of the signal power is sent to the sensor. This signal is further reduced in intensity by the pinhole. The optical interferometer, however, results in having a signal about 36% of the signal from a perfectly reflecting surface. This will allow a lower power source to be utilized in the interferometric system, requiring less power.

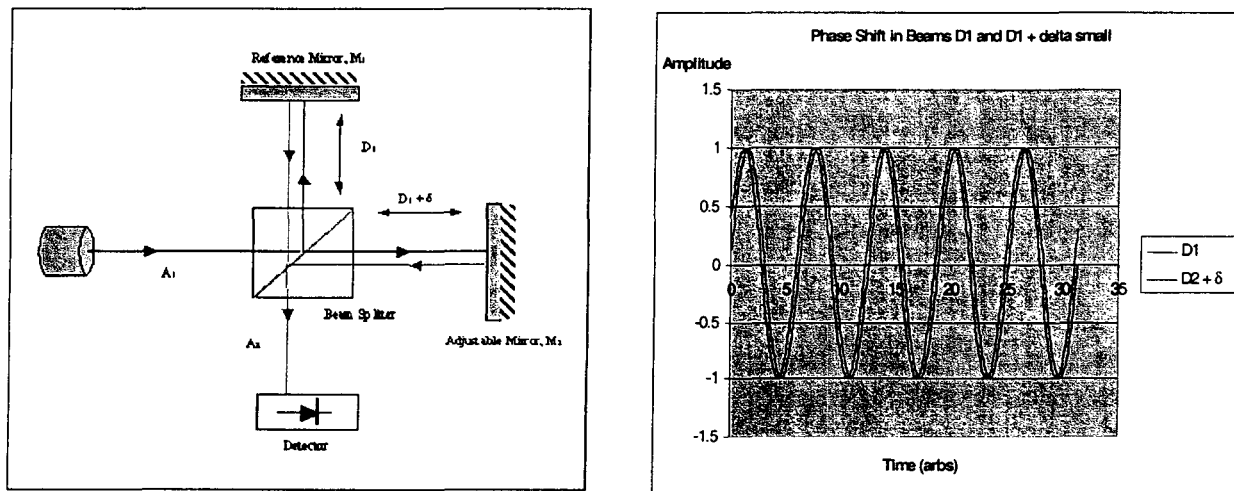
For these reasons it was decided that further development of an interferometric system would be the most promising.

Proof of Concept

In order to meet the requirements for a compact hand held, self contained device, the complexity and power requirements of the current interferometer systems needs to be reduced. First, a low power light source such as a Laser Diode or Light Emitting Diode (LED) can be used in place of a bright white, spatially incoherent source. Next, the complexity of the optics must be reduced as well as the part count. This can be achieved using a simple Michelson interferometer and no microscope objectives or magnification optics. Finally, new techniques to analyze the data must be developed in order to compensate for the removed optics and loss of a dynamically stable platform for one that is hand-held.

A. Finding the Proper Source

In order to find the proper source for the interferometer the concepts of interference and coherence must be understood. Optical interference can be studied using the Michelson interferometer seen below in figure 4.

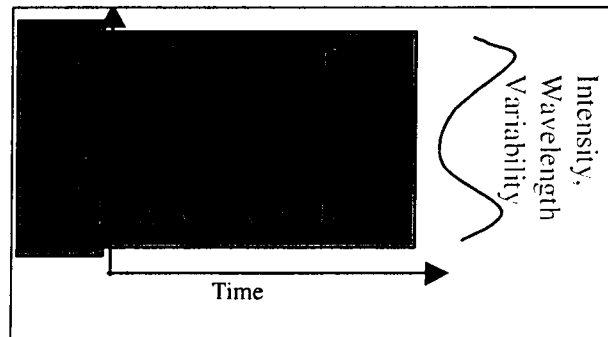


The interferometer consists of a light source, whether it is broad spectrum such as white light or narrow spectrum such as a laser, a beam splitter, two mirrors and a detector. The light beam travels from the source to the beam splitter where the beam is split into approximately two equal intensities. Each beam continues to its respective mirror traveling the distance D_1 to M_1 , or $D_1 + \delta$ to M_2 . The difference in the path length between the two mirrors, δ , affects the intensity of the signal, A_2 , either constructively or destructively. The difference in path length produces a phase shift in the light waves that were split; if the difference δ is zero the waves are in phase and as δ gets larger the waves move out of phase as illustrated in figure 5. The resulting intensity signal for a monochromatic source is given by the following equation E.1:

$$I_f(\tau) = (A_1(t + \tau) + A_1(t))(A_1^*(t + \tau) + A_1^*(t)) \quad \text{E.1}$$

This equation gives the intensity function I_f in terms of the signal amplitude $A_1(\kappa)$ and $A_1^*(\kappa)$ which are complex conjugates of the signal.

Coherence is the degree to which waveforms are related to one another and is closely related to the autocorrelation function. A typical light source has two types of coherence, spatial and temporal. Spatial coherence is the degree of how much a light source is phase coherent across its beam as shown in figure 6 below. Temporal coherence describes the homogeneity along the path of a single wave. As described by Smith & Thompson⁽⁴⁾ the loss of coherence along a path of a wave from a source can be described by considering the wave is made up of a large number of wave trains of finite length. Each



of the wave trains has random phases and made up of a spectrum of frequencies. This leads to the conclusion, and is observed in the laboratory, that in the Michelson interferometer as the path length difference between the two arms is increased the visibility of interference or fringes disappear.

As the signals from the two arms of the interferometer are combined, the autocorrelation or self-coherence function is performed from equation E.1 it can be seen that there are two DC terms and two phase dependant terms that result. The phase dependant terms produce the interference fringes of the interferometer that are represented by equation E.2.

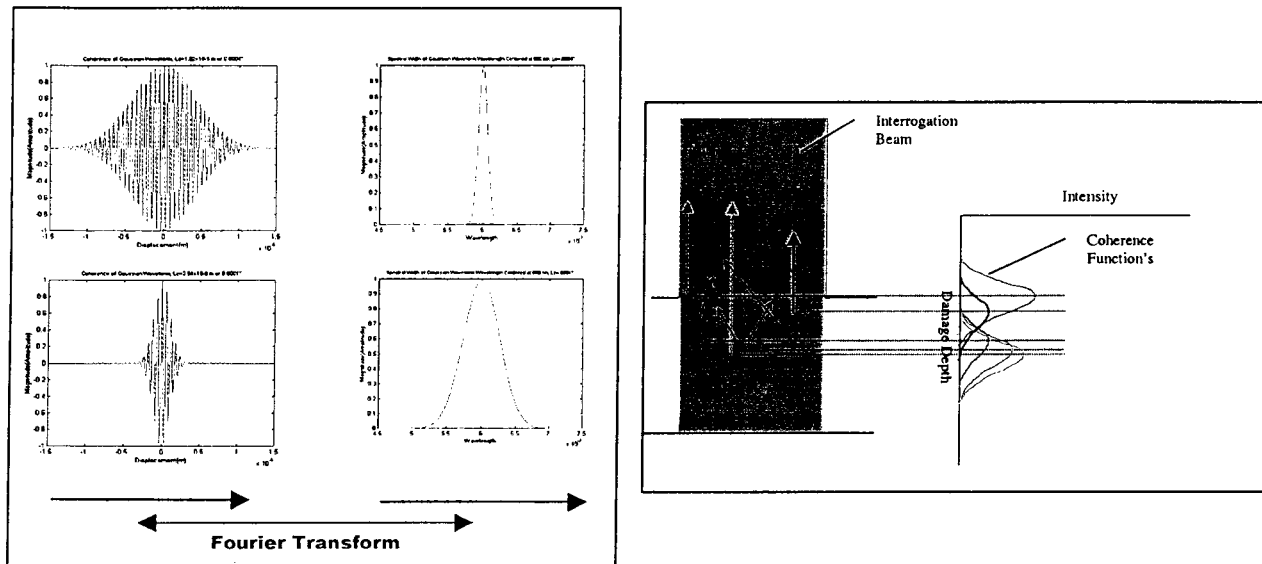
$$\Gamma(\tau) = \langle A_1(t + \tau)A_2^*(t) \rangle \quad \text{E.2}$$

$\Gamma(\tau)$ is the coherence function

$\langle \rangle$ is the time average of the contents in the brackets

The Wiener-Khinchin theorem states that the autocorrelation is equal to the Fourier transform of the square of the magnitude of frequency domain components of A_1 , or the power spectrum of the source signal. Therefore, a source with a broad power spectrum produces a narrow autocorrelation function and vice versa. Figure 7 below show the relation between the light sources power spectrum and the coherence function. The coherence functions are in the left hand side of the figure while the power spectrums are on the right. The coherence functions contain sinusoidal components representing the interference fringes. These fringes are the areas of high correlation with and are the peak amplitudes, while areas of low correlation are the valleys. The x-axis of the coherence function plots represents relative displacement of the reference and sample arms of the interferometer. From this figure, it is obvious that a narrow coherence function would allow the best depth resolution. This would require a broad white source such as a quartz halogen bulb or the like, this proved impractical due to the power restraints. Other low power sources were investigated and it was found that the best sources were laser diodes. Light Emitting Diodes (LED's) were omitted because of their lack of spatial coherence. To broaden the spectrum of the laser diodes the power was reduced under its threshold, this reduced the coherence length from several thousandths of an inch to about one thousandth of an inch. Since we desire resolutions one-tenth this length, measurements will have to be made using the data contained in the interference fringes. A further

concern lies in the fact that by removing the microscope objectives surface roughness of the interrogation area will not be controlled. The approaches to overcoming these and other barriers will be discussed next.

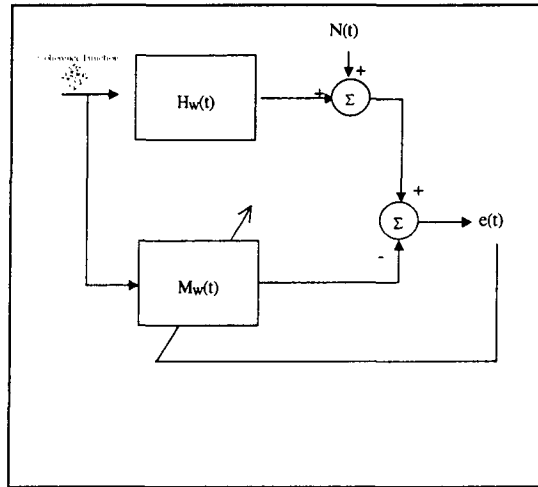


B. Obtaining Useful Signal from a Simplified Profilometer

Due to the limited power spectrum of the laser diode the resulting coherence function is of some finite length, as stated above this coherence length is about 0.001" in length. The coherence function consists of the oscillatory fringes. This presents a problem with multi-convoluted surfaces such as an impact pit that has damage of multiple depths, each producing a coherence function from each surface with a signal intensity proportional to its size (see figure 8). In this figure, it can be seen that a small diameter pit can return a multitude of co-mingled coherence functions that cannot be easily discriminated. Note that in figure 8 the coherence function is represented by the upper half of the functions envelop, this is for ease of illustration. One solution is to decrease the size of the interrogation beam using focusing optics, but these were removed to simplify the design. This figure also indicates that a complete profile of the window contained within the interrogation beam can be collected in a single sweep through the interrogation depth. By utilizing a piezo-mounted mirror the z axis could be scanned rapidly, and using a digital micromirror device to scan in the x-y plane a rapid scanning system could be made. This of course requires a signal processing system to rapidly acquire the signal and analyze the results. Modern Digital Signal Processing (DSP) hardware can be used to process the data once the analysis techniques are developed.

An adaptive signal processing technique called modeling can be used (see figure 9). In this method the error $e(t)$ is minimized by adjusting the coefficients of the math model of the system $M_w(t)$, which will represent the window and any damage it may contain. These coefficients contain the information about the depth and relative size of the damage. In order to produce the most accurate representation of the damage the noise signal $N(t)$ must be understood and reduced to a tolerable level, this is required because the noise signal is added to the interrogation signal of the window $H_w(t)$ and is indistinguishable by the modeling system.

Noise in the system is produced primarily from two sources 1) electronic noise in the data acquisition system and 2) noise caused by system vibration. In their paper titled Analysis of measurement accuracy in sinusoidal phase modulating interferometry, O. Sasaki and H. Okazaki⁽⁷⁾ conclude that the noise caused by system mechanical vibration is multiplicative and noise caused by system electronics is additive this is represented in the following equation E.3



$$s(t) = s_0 \cos[z \cos(w_c t + \phi) + \alpha + n_M(t)] + n_A(t)$$

E.3

Here the signal $s(t)$ is produced by sinusoidally modulating the reference arm of the interferometer about the area of coherence. The term $n_M(t)$ is the multiplicative noise and $n_A(t)$ is the additive noise. Sinusoidal modulation of the coherence function is a common technique to reduce noise caused by extraneous light sources and allows high noise rejection by using a filter centered about the modulation frequency or one of its harmonics. This sinusoidal modulation/filter technique significantly reduces the multiplicative and additive noise assuming the multiplicative noise is zero mean Gaussian. To make these assumptions all vibrational noise that is not Gaussian must be eliminated by mounting and isolation techniques in optics of the system. Once the noise is reduced to acceptable levels the analysis of the data will consist of deciphering the model $M_w(t)$. Since the interrogation spot size is of some finite three-dimensional dimension an area with window damage such as a pit or scratch can contain many convoluted signal returns. Therefore, interrogation methods are being explored to remove ambiguity in the data. The methods being explored consist of interrogating from a multitude of angles and overlapping scans and the use of DMD.

Continuing Work

Work is continuing in using the adaptive filter to model the damaged window, using the sinusoidal modulation/filter technique. Currently improvements are being made in the data acquisition and filtering methods so that better models may be produced. Future work will involve the investigation of interrogation methods and the implementation of the rapid scanning of the x-y and z-axis and development of the associated software.

References

1. G.Q. Xiao, T.R. Corle and G.S. Kino, Real-time confocal scanning optical microscope, Appl. Phys. Lett. 53 (8), 716 – 718 (1988)
2. S. Cha, P.C. Lin, L. Zhu, E.L. Botvinick, P.C. Sun, Y. Fainman, 3D profilometry using a dynamically configurable confocal microscope, University of California/San Diego, Dept. of Electrical and Computer Engineering (available at www-bioeng.ucsd.edu/~ebotvini/SPIE99.html)
3. J.C. Wyant, J. Schmit, Large Field of View, High Spatial Resolution, Surface Measurements, International Journal of Machine Tools Manufacturers, Vol. 38, Page 691 (1998)
4. F.G. Smith- J.H. Thompson, Optics, 2nd ed., John Wiley and Sons, 1971, 1988
5. L. Deck, P. de Groot, High-speed noncontact profiler based on scanning white-light interferometry, Applied Optics, Vol. 33, No. 31, 1994
6. R. Youngquist, R. Wentworth, K. Fesler, Selective interferometric sensing by the use of coherence synthesis, Optics Letters, Vol. 12, page 944, 1987
7. O. Sasaki and H. Okazaki, Analysis of measurement accuracy in sinusoidal phase modulating interferometry, Applied Optics, Vol. 25, No. 18, September 1986